


ORIGINAL RESEARCH

Cross talk between β subunits, intracellular Ca^{2+} signaling, and SNAREs in the modulation of $\text{Ca}_v2.1$ channel steady-state inactivation

Selma Angèlica Serra, Gemma G. Gené[†], Xabier Elorza-Vidal & José M. Fernández-Fernández* 

Laboratori de Fisiologia Molecular, Departament de Ciències Experimentals i de la Salut, Universitat Pompeu Fabra, Barcelona, Spain

Keywords

Ca^{2+} -calmodulin, $\text{Ca}_v2.1$ domains for SNARE-mediated modulation, $\text{Ca}_v2.1$ steady-state inactivation, $\text{Ca}_v\beta$ subunits, presynaptic voltage-gated $\text{Ca}_v2.1$ channels, syntaxin-1A.

Correspondence

José M. Fernández-Fernández, Laboratory of Molecular Physiology, Universitat Pompeu Fabra, C/ Dr. Aiguader 88, Barcelona 08003, Spain.

Tel: 34 93 3160854

Fax: 34 93 3160901

E-mail: jmanuel.fernandez@upf.edu

Funding Information

This work was supported by the Spanish Ministry of Economy and Competitiveness (Grants SAF2012-31089 and SAF2015-69762-R to JMF-F, and Grant MDM-2014-0370 through the "María de Maeztu" Programme for Units of Excellence in R&D to "Departament de Ciències Experimentals i de la Salut"), and FEDER Funds.

Received: 22 September 2017; Revised: 23 November 2017; Accepted: 3 December 2017

doi: 10.14814/phy2.13557

Physiol Rep, 6 (2), 2018, e13557,
<https://doi.org/10.14814/phy2.13557>

[†]Deceased March 31, 2017

Key points summary

- The functional interaction between presynaptic voltage-gated Ca^{2+} channels ($\text{Ca}_v2.x$) and soluble N-ethylmaleimide-sensitive factor attachment protein receptor

Abstract

Modulation of $\text{Ca}_v2.1$ channel activity plays a key role in interneuronal communication and synaptic plasticity. SNAREs interact with a specific *synprint* site at the second intracellular loop (LII-III) of the $\text{Ca}_v2.1$ pore-forming α_{1A} subunit to optimize neurotransmitter release from presynaptic terminals by allowing secretory vesicles docking near the Ca^{2+} entry pathway, and by modulating the voltage dependence of channel steady-state inactivation. Ca^{2+} influx through $\text{Ca}_v2.1$ also promotes channel inactivation. This process seems to involve Ca^{2+} -calmodulin interaction with two adjacent sites in the α_{1A} carboxyl tail (C-tail) (the IQ-like motif and the Calmodulin-Binding Domain (CBD) site), and contributes to long-term potentiation and spatial learning and memory. Besides, binding of regulatory β subunits to the α interaction domain (AID) at the first intracellular loop (LI-II) of α_{1A} determines the degree of channel inactivation by both voltage and Ca^{2+} . Here, we explore the cross talk between β subunits, Ca^{2+} , and syntaxin-1A-modulated $\text{Ca}_v2.1$ inactivation, highlighting the α_{1A} domains involved in such process. β_3 -containing $\text{Ca}_v2.1$ channels show syntaxin-1A-modulated but no Ca^{2+} -dependent steady-state inactivation. Conversely, β_{2a} -containing $\text{Ca}_v2.1$ channels show Ca^{2+} -dependent but not syntaxin-1A-modulated steady-state inactivation. A LI-II deletion confers Ca^{2+} -dependent inactivation and prevents modulation by syntaxin-1A in β_3 -containing $\text{Ca}_v2.1$ channels. Mutation of the IQ-like motif, unlike CBD deletion, abolishes Ca^{2+} -dependent inactivation and confers modulation by syntaxin-1A in β_{2a} -containing $\text{Ca}_v2.1$ channels. Altogether, these results suggest that LI-II structural modifications determine the regulation of $\text{Ca}_v2.1$ steady-state inactivation either by Ca^{2+} or by SNAREs but not by both.

(SNARE) proteins of the secretory machinery, optimizes neurotransmitter-mediated interneuronal communication.

- Alteration of such functional interaction has clinical relevance in the context of neurological disorders such as ataxia and migraine.

- Regardless of the important anchoring function of a specific Ca_v2.x region (the *synprint* site) in the Ca_v2.x-SNAREs interaction, the involvement of other channel domains has been proposed.
- By combining heterologous expression in HEK 293 cells, whole-cell patch-clamp and site-directed mutagenesis, we show that Ca_v2.1-SNAREs functional interaction entails Ca_v2.1 molecular determinants beyond the *synprint* site, including the first intracellular loop and the carboxyl tail, and their physical interaction with regulatory β subunits and the Ca²⁺-calmodulin complex, respectively.
- Altogether help us better understand the molecular machinery that initiates and regulates vesicles fusion with the presynaptic plasma membrane to trigger chemical neurotransmission.

Introduction

Ca²⁺ entry through the high-voltage-activated (HVA) Ca_v2.x channels (mainly Ca_v2.1 [P/Q-type] channels) into presynaptic nerve terminals supports a transient Ca²⁺ microdomain that is essential for synaptic exocytosis leading to the fast release of classical neurotransmitters (Catterall 2011). To ensure fast and efficient neurotransmitter release, the vesicle-docking/release machinery must be located near the pathway of Ca²⁺ entry. In many cases, this close localization is achieved by direct interaction of soluble N-ethylmaleimide-sensitive factor attachment protein receptor (SNARE) proteins with the Ca²⁺ channel pore-forming α_1 subunit, which consists of four repeated domains (I–IV) each containing six transmembrane regions (S1–S6) with a voltage sensor (S1–S4) and a pore region (S5, P-loop, and S6). Indeed, syntaxin-1A/1B, SNAP-25, and synaptotagmin-1 specifically interact with Ca_v2.1 and Ca_v2.2 channels by binding to a synaptic protein interaction site (*synprint*) located within the intracellular loop connecting domains II and III (LII–III) of the channels (Sheng et al. 1994, 1997; Rettig et al. 1996; Kim and Catterall 1997; Jarvis et al. 2002) (Fig. 1A). Furthermore, it has been suggested that exocytosis is activated even before Ca²⁺ entry, by conformational changes triggered during Ca²⁺ binding at the open Ca_v channel pore, which are transmitted from the channel to specific residues of Ca_v-interacting SNARE proteins, accounting for the rapid time frame of evoked release (Atlas 2013; Bachnoff et al. 2013). Whichever the case, perhaps an equally important consequence of SNARE protein interaction with the Ca²⁺ channel is the modulation of presynaptic Ca²⁺ channel activity, thus fine-tuning the amount of Ca²⁺ that binds to the pore, enters the synaptic terminal, and determines synaptic transmission strength. Specifically, the binding of syntaxin-1A and SNAP-25 to Ca_v2.1 and

Ca_v2.2 α_1 subunits shifts the voltage dependence of steady-state inactivation toward more negative membrane potentials following trains of brief depolarizing pulses to reduce channel availability, without affecting channel activation properties (Bezprozvanny et al. 1995; Zhong et al. 1999). Such inhibition is reverted, and channel activity fully restored, by synaptotagmin (Zhong et al. 1999). Thus, Ca_v2.x-SNAREs interaction seems to optimize neurotransmission by favoring Ca²⁺ entry through channels presenting docked synaptic vesicles. Accordingly, the disruption of such functional interaction compromises not just vesicle exocytosis in vitro (Mochida et al. 2003; Harkins et al. 2004), but also synaptic transmission and the SNARE-mediated inhibitory modulation of Ca_v2.x channels in vivo (Mochida et al. 1996; Rettig et al. 1997; Zamponi 2003; Keith et al. 2007). Moreover, human α_{1A} mutations impairing the functional interaction between Ca_v2.1 channels and SNARE proteins have clinical relevance in the context of ataxia and the phenotypic expression of both migraine with aura and hemiplegic migraine (Cricchi et al. 2007; Serra et al. 2010; Condliffe et al. 2013).

Beyond the important anchoring function of the *synprint* site in the SNARE-mediated modulation of Ca_v2.x channel gating, the involvement of other molecular domains has been proposed. Hence, deletions within the LII–III intracellular loop of the Ca_v2.2 α_{1B} channel subunit that completely eliminate the *synprint* site reduce but not abolish channel modulation by syntaxin, and syntaxin mutations that have no effect on binding affinity to α_{1B} -*synprint* prevent the SNARE-mediated regulation of Ca_v2.2 channel inactivation (Bezprozvanny et al. 2000). Besides, the A454T mutation (placed in the intracellular loop connecting domains I and II (LI–II) of the Ca_v2.1 α_{1A} channel subunit, and associated to both early-onset progressive ataxia (Cricchi et al. 2007) and the relief of migraine aura symptoms (Serra et al. 2010)) prevents the negative modulation of Ca_v2.1 channels by SNARE proteins and decreases channel coupling to exocytosis, thus revealing the importance of LI–II structural integrity in the Ca_v2.1-SNAREs functional interaction (Serra et al. 2010).

The molecular mechanism by which LI–II influences Ca_v2.1-SNAREs functional interaction is unknown. However, it is well established that LI–II plays a determinant role in the regulation of Ca_v2.1 channel activity (Buraei and Yang 2010). In this sense, it has been suggested that conformational changes induced at LI–II by the binding of functionally different regulatory β subunits not only determine the degree of voltage-dependent inactivation but also the extent of a Ca²⁺-dependent inactivation component (mediated by the binding of Ca²⁺-calmodulin to two adjacent sites in the carboxyl tail [C-tail] of the α_{1A} subunit: the IQ-like motif and the Calmodulin-Binding Domain [CBD] site) (Lee et al. 2000; DeMaria et al.

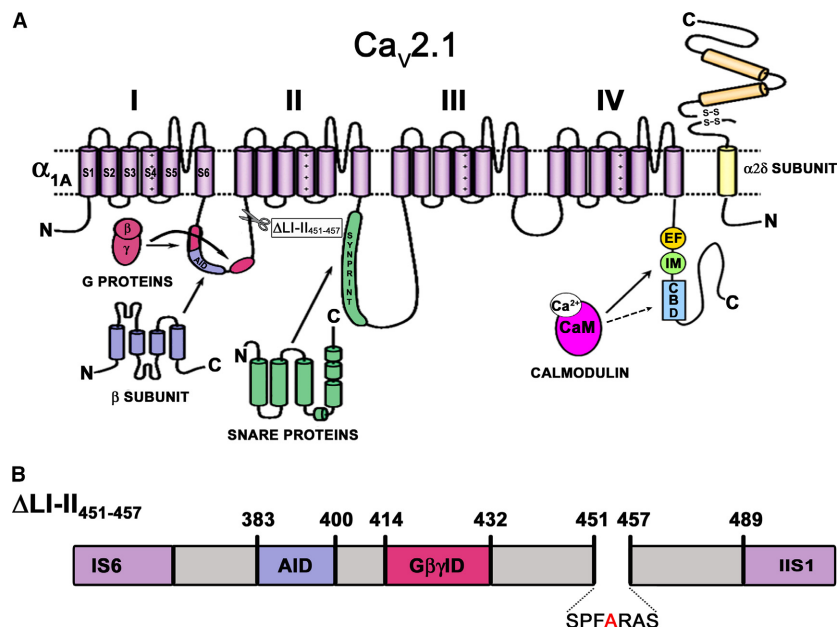


Figure 1. Location of the known α_{1A} molecular determinants for the binding of the main intracellular proteins that modulate Ca_v2.1 channel inactivation. (A) Schematic representation of the secondary structure of the Ca_v2.1 α_{1A} channel subunit, showing the location of the known α_{1A} molecular determinants for the binding of three cytosolic proteins involved in the regulation of Ca_v2.1 channel inactivation: (1) regulatory β subunits (which binds to the α -interaction domain or AID, located in the cytoplasmic loop connecting domains I and II (LI-II) of α_{1A}); (2) SNARE proteins (that interacts with the *synprint* site, within the intracellular loop connecting domains II and III (LII-III) of α_{1A}); and (3) the Ca²⁺-calmodulin (Ca²⁺-CaM) complex (which binds to the IQ-like motif and the Calmodulin-Binding Domain (CBD) site, at the carboxyl tail of α_{1A}). (B) Location of the α_{1A} LI-II deletion around the A454 residue (Δ LI-II₄₅₁₋₄₅₇) (also depicted at panel A).

2001; Cens et al. 2006) (Fig. 1A). Interestingly, disruption of Ca_v2.1 modulation by calmodulin and related Ca²⁺ sensor proteins by mutation of the IQ-like motif has been reported to impair long-term potentiation and spatial learning and memory in mice (Nanoua et al. 2016).

Altogether, it draws a complex scenario in which Ca_v2.1 inactivation is produced by LI-II and modulated by: β channel subunits interacting with LI-II, SNARE proteins binding to the *synprint* site at the LII-III but requiring the integrity of LI-II, and Ca²⁺-calmodulin attached to the C-tail of the α_{1A} subunit.

To better understand the role of LI-II in Ca_v2.1-SNAREs functional interaction, we analyzed the modulation of Ca_v2.1 inactivation by syntaxin-1A under intermediate and high Ca²⁺-buffering conditions, in the presence of functionally different regulatory β subunits (β_{2a} or β_3) and distinct human α_{1A} constructs containing either a LI-II deletion around the A454 residue, mutations in the IQ-like region, or a CBD deletion. Our results reveal a cross talk between different pathways involved in the modulation of Ca_v2.1 inactivation, showing that regulation by syntaxin-1A of the human Ca_v2.1 channel activity requires both the integrity of α_{1A} LI-II and the lack of a Ca²⁺-dependent component in the channel steady-state inactivation.

Methods

cDNA constructs and site-directed mutagenesis

cDNA of the human voltage-gated Ca²⁺ (Ca_v2.1) channel α_{1A} subunit (originally cloned into a pCMV vector) was a gift from Professor J. Striessnig (University of Innsbruck, Austria). cDNAs of the rabbit $\alpha_2\delta$ and rat β_3 and β_{2a} regulatory subunits, and syntaxin-1A (subcloned into a pcDNA3 expression vector) were gifts from Dr. L. Birnbaumer (National Institutes of Health, North Carolina, USA) and Dr. J. Blasi (Universitat de Barcelona, Spain). Ca_v2.1 α_{1A} mutant subunits (Δ LI-II₄₅₁₋₄₅₇, IM/EE_{1964;1965}, Δ CBD_{2020-end}) were generated using site-directed mutagenesis (GenScript Corporation, Piscataway, NJ). All cDNA clones used in this study were sequenced in full to confirm their integrity.

Heterologous expression and electrophysiology

HEK 293 cells were transfected using a linear polyethylenimine (PEI) derivative, the polycation ExGen500 (Fermentas Inc., Hanover, Maryland, USA) as previously

reported (eight equivalents PEI/3.3 μg DNA/dish) (Serra et al. 2010). For transfection, α_{1A} (wild-type [WT] or mutants), β₃ or β_{2a}, α_{2δ}, and EGFP (transfection marker) cDNA constructs were used at a ratio of 1:1:1:0.3. When required, syntaxin-1A was also cotransfected at the same ratio as Ca_v2.1 channel subunit cDNAs. Electrophysiological recordings were obtained from EGFP-positive cells 24–48 h after transfection at room temperature (22–24°C).

Ca²⁺ currents (I_{Ca²⁺}) through WT or mutant Ca_v2.1 channels containing β₃ or β_{2a} regulatory subunits were recorded in the whole-cell configuration of the patch-clamp technique, using a D-6100 Darmstadt amplifier (List Medical, Germany). Pipettes had a resistance of 2–3 MΩ when filled with a solution containing (in mmol/L): 140 CsCl, 1 EGTA (intermediate Ca²⁺-buffering condition) or 10 BAPTA (high Ca²⁺-buffering condition), 4 Na₂ATP, 0.1 Na₃GTP, and 10 Hepes (pH 7.2–7.3 and 290–300 mOsmol/L). The external solution contained (in mmol/L): 140 tetraethylammonium-Cl (TEACl), 3 CsCl, 2.5 CaCl₂, 1.2 MgCl₂, 10 Hepes, and 10 D-glucose (pH 7.4 and 300–310 mOsmol/L). Previous work demonstrates that high levels of intracellular Ca²⁺ chelators (e.g., 10 mmol/L EGTA or 10 mmol/L BAPTA) impair Ca_v2.1 inactivation in a similar way as when replacing extracellular Ca²⁺ by Ba²⁺ (Lee et al. 2000). Such observation strongly suggest that chelator effect is due to Ca²⁺ buffering, ruling out any unwanted direct action of the Ca²⁺ chelator itself on channel inactivation. pClamp8 software (Molecular Devices, USA) was used for pulse generation, data acquisition, and subsequent analysis.

Steady-state inactivation was estimated by measuring peak Ca²⁺ currents in response to a 50 ms (or 10 ms, when using the α_{1A} IM/EE mutant subunit) depolarizing test pulse (to +20 mV) from a holding of –80 mV, following 30-sec steps to various holding potentials

(conditioning pulses) between –80 and +20 mV (Fig. 1A). Between the 30-sec conditioning depolarizations and the test pulse we employed a 20-msec interpulse to the holding potential, which does not allow detectable recovery from inactivation of Ca_v2.x channels (Degtiar et al. 2000). This kind of protocol has been reported to detect significant increase in Ca_v2.x steady-state inactivation induced by syntaxin-1A (i.e., a left shift of V_{1/2 inact} to more negative voltages by ~6 mV) (Degtiar et al. 2000). On the contrary, when using shorter (few seconds) conditioning pulses, the influence of syntaxin-1A on Ca_v2.x channel gating was barely detectable (Degtiar et al. 2000). These results are consistent with the action of SNAREs on slow rather than fast channel inactivation (Degtiar et al. 2000). As described in detail previously (Serra et al. 2010), normalized I_{Ca²⁺} persistent currents were fitted to the following Boltzmann equation in order to obtain half-maximal voltage (V_{1/2 inact}) and slope factor (k_{inact}) for steady-state inactivation:

$$\frac{I}{I_{\max}} = \frac{1}{1 + e^{\frac{V - V_{1/2 \text{ inact}}}{k_{\text{inact}}}}} \quad (1)$$

Statistics

Data are presented as the means ± SEM, and *n* represents the number of cells recorded for each experimental condition. Statistical significance was tested using one-way Analysis of Variance (ANOVA) followed by a Bonferroni post hoc test. Differences were considered significant if *P* < 0.05. All statistical comparisons were performed using the GraphPad Instat software. All data are sampled from Gaussian (normal) distributions (tested using the method Kolmogorov and Smirnov).

Figure 2. Steady-state inactivation of Ca_v2.1 channels containing the regulatory β₃ subunit is independent of intracellular Ca²⁺ signaling and is favored by syntaxin-1A (A) Voltage protocol for the study of Ca_v2.1 channels steady-state inactivation (see Methods for further details). Representative normalized Ca²⁺ current traces recorded at intermediate (1 mmol/L EGTA) (B) or high (10 mmol/L BAPTA) (C) intracellular Ca²⁺-buffering conditions from a HEK 293 cell expressing Ca_v2.1 channels composed of wild-type α_{1A}, β₃, and α_{2δ} subunits (WTβ₃) either in the absence (left) or presence (right) of syntaxin-1A (stx 1A). Currents were elicited by 50 ms depolarizing steps to +20 mV applied after 30-sec depolarizing prepulses to the indicated voltages. Amplitudes of currents elicited by test pulses to +20 mV after the different prepulses were normalized to the maximum current amplitude obtained after a 30-sec prepulse to –80 mV in order to generate the corresponding mean steady-state inactivation curves (D), which were fitted to a single Boltzmann function (see Methods, eq. 1) to estimate the half-inactivation potentials (V_{1/2 inactivation}) (E) for WT Ca_v2.1 channels containing the β₃ subunit (WTβ₃) in the absence (open circles) or presence (filled circles) of syntaxin-1A (stx 1A), at the above indicated intracellular Ca²⁺-buffering conditions. Average V_{1/2 inact} and k_{inact} values at intermediate Ca²⁺-buffering condition (1 mmol/L EGTA) were (in mV): WTβ₃ (open circles, *n* = 18) –23.7 ± 0.83 and –5.16 ± 0.24; WTβ₃ + stx 1A (filled circles, *n* = 12) –32.74 ± 1.46 and –5.5 ± 0.19, respectively. At high Ca²⁺-buffering condition (10 mmol/L BAPTA), average V_{1/2 inact} and k_{inact} values were (in mV): WTβ₃ (open circles, *n* = 12) –20.74 ± 1.18 and –4.78 ± 0.16; WTβ₃ + stx 1A (filled circles, *n* = 8) –25.68 ± 1.13 and –5.25 ± 0.21, respectively. a and b: *P* < 0.001 and *P* < 0.05 versus the corresponding control condition (absence of syntaxin-1A), respectively; c: *P* < 0.01 when compared to the intermediate Ca²⁺-buffering condition (1 mmol/L EGTA). No significant difference was found for k_{inact} values (ANOVA *P* = 0.17).

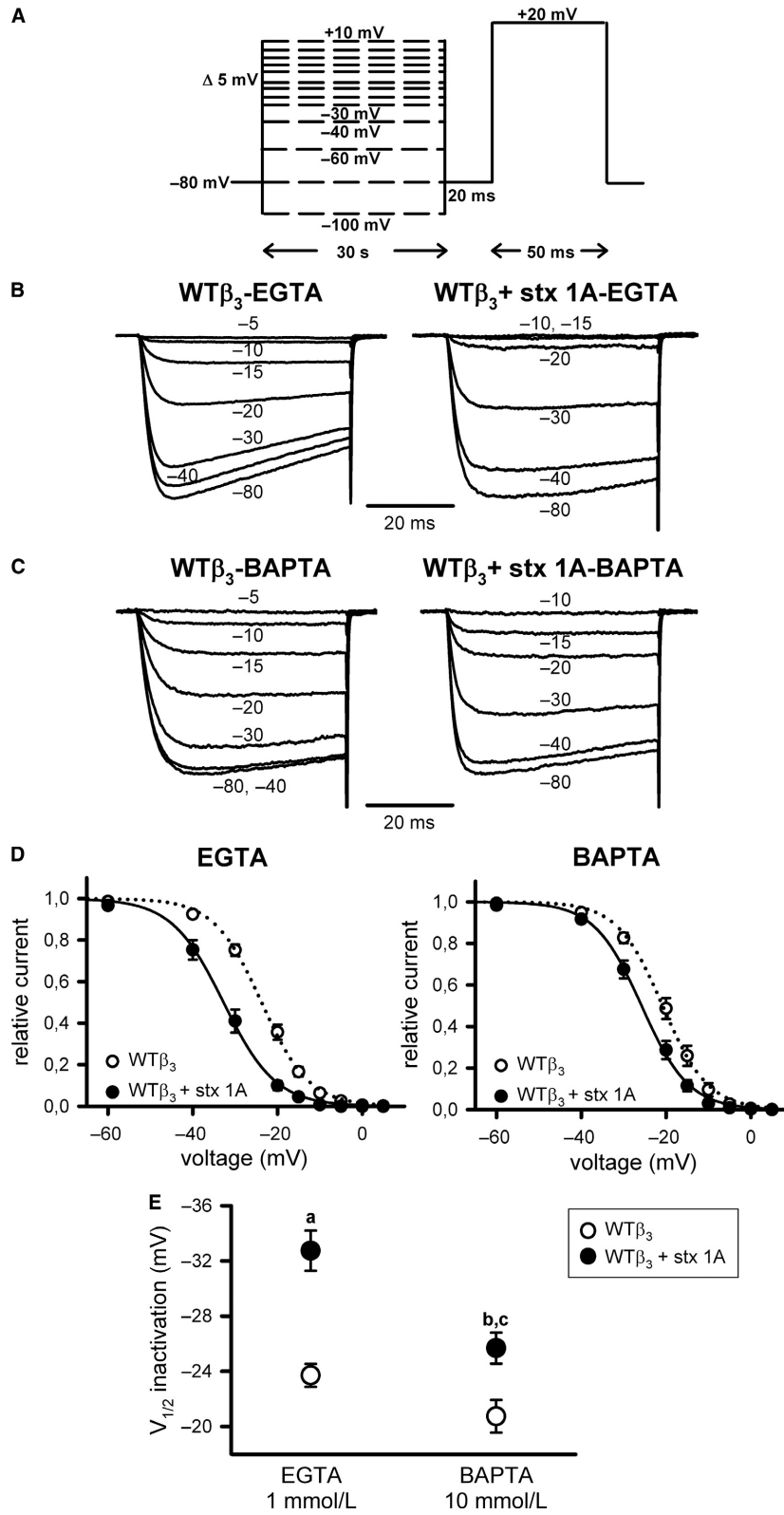


Table 1. Summary of half-maximal voltage for steady-state inactivation ($V_{1/2}$ inact) values of the different Ca_v2.1 channels analyzed under intermediate (1 mM EGTA) and high (10 mM/L BAPTA) Ca²⁺-buffering conditions in the absence (–stx 1A) or presence (+stx 1A) of syntaxin-1A

Ca _v 2.1 channel	1 mmol/L EGTA		10 mmol/L BAPTA	
	–stx 1A	+stx 1A	–stx 1A	+stx 1A
WTβ ₃	–23.7 ± 0.83 (n = 18)	–32.74 ± 1.46*** (n = 12)	–20.74 ± 1.18 (n = 12)	–25.68 ± 1.13 */** (n = 8)
ΔLI-IIβ ₃	–29.58 ± 1.35 (n = 14)	–30 ± 1.85 (n = 9)	–21.84 ± 0.83*** (n = 9)	–27.94 ± 1.15* (n = 8)
WTβ _{2a}	–12.08 ± 1.36 (n = 12)	–14.53 ± 1.02 (n = 11)	–2.78 ± 0.95*** (n = 9)	–7.57 ± 1.36*/*** (n = 11)
ΔLI-IIβ _{2a}	–11.47 ± 0.86 (n = 8)	–13.57 ± 1.15 (n = 9)	–2.58 ± 0.99*** (n = 9)	–7.45 ± 1.15*/*** (n = 9)
IM/EEβ _{2a}	4.19 ± 0.8 (n = 10)	–1.25 ± 1.71* (n = 11)	1.4 ± 0.95 (n = 7)	–4.68 ± 1.71* (n = 9)
ΔCBDβ _{2a}	–12.48 ± 1.07 (n = 8)	–14.75 ± 1.53 (n = 6)	–4.43 ± 1.15** (n = 12)	–9.6 ± 1.61* (n = 12)

Data are presented as the means ± S.E.M, and *n* represents the number of cells recorded for each experimental condition.

Red asterisks for significant increases (left shift of $V_{1/2}$ inact to more negative voltages) in channel steady-state inactivation induced by syntaxin-1A versus the corresponding control condition (absence of syntaxin-1A). Blue asterisks for significant decreases (right shift of $V_{1/2}$ inact to less negative voltages) in channel steady-state inactivation induced by high Ca²⁺ buffering when compared to the corresponding intermediate Ca²⁺-buffering condition (1 mM/L EGTA). (ANOVA followed by a Bonferroni post hoc test).

P* < 0.05, *P* < 0.01, and ****P* < 0.001.

Results

The impact of the SNARE protein syntaxin-1A on the steady-state inactivation of Ca²⁺ currents ($I_{Ca^{2+}}$) through wild-type (WT) Ca_v2.1 channel containing the regulatory β₃ subunit (WTβ₃), was measured at intermediate (1 mM/L EGTA) and high (10 mM/L BAPTA) intracellular Ca²⁺-buffering conditions to evaluate its calcium dependency. In both conditions, syntaxin-1A expression favored channel steady-state inactivation, as indicated by a significant left shift of $V_{1/2}$ inact to more negative voltages (by ~5–9 mV) (Fig. 2B–E; Table 1). It must be noted that steady-state inactivation of WTβ₃ channels was poorly dependent on intracellular Ca²⁺ concentration, as not significant differences were found when comparing $I_{Ca^{2+}}$ $V_{1/2}$ inact values obtained at intermediate and high intracellular Ca²⁺-buffering conditions in the absence of syntaxin-1A (Fig. 2B and C (left panels), D and E (open circles); Table 1).

Interestingly, the introduction of a small deletion around the A454 residue at the first intracellular loop of the pore-forming α_{1A} subunit (ΔLI-II_{451–457}) (Fig. 1) made the steady-state inactivation of β₃-containing Ca_v2.1 channels (ΔLI-IIβ₃) Ca²⁺-dependent. On one hand, $I_{Ca^{2+}}$ inactivation was reduced (with a significant ~8 mV right shift in the $V_{1/2}$ inact) by increasing the buffering of intracellular Ca²⁺ (Fig. 3A and B (left panels), C and D (open circles); Table 1). On the other hand, such α_{1A}

LI-II deletion removed the modulatory action of syntaxin-1A on the steady-state inactivation of Ca_v2.1 channels containing β₃ at intermediate Ca²⁺-buffering condition (Fig. 3A, C [left panel], and D; Table 1), when Ca²⁺ entry through the channel promotes inactivation. The effect of syntaxin-1A on the inactivation of the ΔLI-IIβ₃ channel was recovered ($V_{1/2}$ inact was significantly left-shifted by ~6 mV) by increasing intracellular Ca²⁺ buffering to abrogate the novel LI-II deletion-induced Ca²⁺-dependent component of inactivation (Fig. 3B and C [right panel], D; Table 1).

As widely reported before (for a review see Buraei and Yang 2010), Ca_v2.1 inactivation was substantially right-shifted to more depolarized potentials for β_{2a}-containing than for β₃-containing channels (Fig. 4 vs. Fig. 2; Table 1). Under this condition, unlike WTβ₃ channels, the steady-state inactivation of $I_{Ca^{2+}}$ through the β_{2a}-containing WT Ca_v2.1 channel (WTβ_{2a}) presented a Ca²⁺-dependent component (Fig. 4) that is not affected by the deletion in the first intracellular loop of the α_{1A} subunit (ΔLI-II_{451–457}) (Fig. 5). Thus, $V_{1/2}$ inact was significantly shifted to less negative values for both WTβ_{2a} and ΔLI-IIβ_{2a} channels (by ~9 mV) when increasing intracellular Ca²⁺ buffering (Fig. 4A and B (left panels), C and D (open circles); Fig. 5A and B (left panels), C and D (open circles); Table 1). Accordingly, such right shift in the voltage dependence of inactivation disappeared once the β_{2a}-containing Ca_v2.1 channel was rendered insensitive to

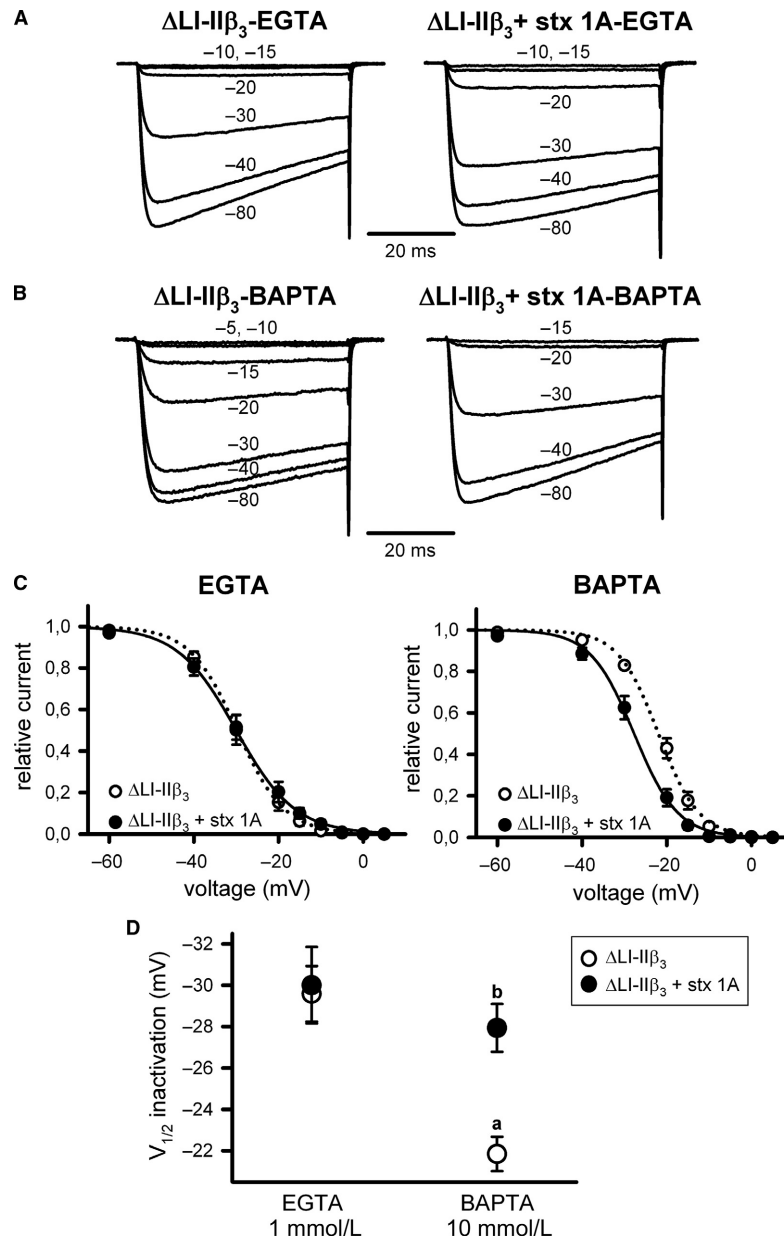


Figure 3. $\Delta 451\text{-}457$ at α_{1A} LI-II promotes a Ca²⁺-dependent component in the steady-state inactivation of Ca_v2.1 channels containing the auxiliary β_3 subunit, and it prevents syntaxin-1A-mediated modulation. Typical normalized Ca²⁺ current traces recorded at intermediate (1 mmol/L EGTA) (A) or high (10 mmol/L BAPTA) (B) intracellular Ca²⁺-buffering conditions from a HEK 293 cell expressing Ca_v2.1 channels composed of mutant $\Delta\text{LI-II}_{451\text{-}457}$ α_{1A} , β_3 , and $\alpha_2\delta$ subunits ($\Delta\text{LI-II}\beta_3$) either in the absence (left) or presence (right) of syntaxin-1A (stx 1A). Currents were elicited by 50-ms depolarizing steps to +20 mV applied after 30-sec depolarizing prepulses to the shown voltages. Corresponding mean normalized steady-state inactivation curves (C), and derived $V_{1/2}$ inactivation (D) for $\Delta\text{LI-II}_{451\text{-}457}$ Ca_v2.1 mutant channels containing the β_3 subunit ($\Delta\text{LI-II}\beta_3$) in the absence (open circles) or presence (filled circles) of syntaxin-1A (stx 1A), at the above indicated intracellular Ca²⁺-buffering conditions. Average $V_{1/2}$ inact and k_{inact} values at intermediate Ca²⁺-buffering condition (1 mmol/L EGTA) were (in mV): $\Delta\text{LI-II}\beta_3$ (open circles, $n = 14$) -29.58 ± 1.35 and -4.73 ± 0.16 ; $\Delta\text{LI-II}\beta_3 + \text{stx 1A}$ (filled circles, $n = 9$) -30 ± 1.85 and -5.73 ± 0.35 , respectively. At high Ca²⁺-buffering condition (10 mmol/L BAPTA), average $V_{1/2}$ inact and k_{inact} values were (in mV): $\Delta\text{LI-II}\beta_3$ (open circles, $n = 9$) -21.84 ± 0.83 and -4.94 ± 0.47 ; $\Delta\text{LI-II}\beta_3 + \text{stx 1A}$ (filled circles, $n = 8$) -27.94 ± 1.15 and -4.97 ± 0.33 , respectively. a: $P < 0.001$ when compared to the intermediate Ca²⁺-buffering condition (1 mmol/L EGTA); b: $P < 0.05$ versus the corresponding control condition (absence of syntaxin-1A). No significant difference was found for k_{inact} values (ANOVA $P = 0.14$).

Ca²⁺ by the introduction of a double mutation (IM to EE) at the calmodulin-binding IQ-like motif (Fig. 6A and B [left panels], C and D [open circles]; Table 1). Modulation by syntaxin-1A of WT β_{2a} and Δ LI-II β_{2a} I_{Ca}²⁺ steady-state inactivation was occluded when the Ca²⁺-dependent component was present (Fig. 4A and C [left panel], D; Fig. 5A and C [left panel], D; Table 1). Syntaxin-1A-induced left shift of $V_{1/2 \text{ inact}}$ (by \sim 5–6 mV) was only present when the Ca²⁺-dependent component of the steady-state inactivation of β_{2a} -containing Ca_v2.1 channels was removed, either by increasing intracellular Ca²⁺ buffering (Fig. 4B and C [right panel], D; Fig. 5B and C [right panel], D; Table 1) or by introducing the IM/EE double mutation at the IQ-like motif (Fig. 6A–D; Table 1).

Truncation of the α_{1A} carboxyl tail, downstream the IQ-like motif, to fully remove the distal calmodulin-binding domain (CBD) site of the β_{2a} -containing Ca_v2.1 channel (Δ CBD β_{2a}) did not eliminate the Ca²⁺-dependent component of I_{Ca}²⁺ steady-state inactivation, and $V_{1/2 \text{ inact}}$ was still significantly shifted to less negative values (by \sim 9 mV) when increasing intracellular Ca²⁺ buffering (Fig. 7A and B (left panels), C and D (open circles); Table 1). At intermediate intracellular Ca²⁺ buffering, the presence of the Ca²⁺-dependent component in the steady-state inactivation of Δ CBD β_{2a} channels hindered their modulation by syntaxin-1A (Fig. 7A and C (left panel), D; Table 1), and the SNARE protein only shifted $V_{1/2 \text{ inact}}$ to more negative potentials (by \sim 5 mV) under high intracellular Ca²⁺ buffering (Fig. 7B and C (right panel), D; Table 1).

Discussion

Taken together, our results bring to light a functional cross talk between three different signaling pathways regulating Ca_v2.1 channel steady-state inactivation: (1) regulatory β subunits through their interaction with the α interaction domain (AID) located at the first intracellular loop (LI-II) of the Ca_v2.1 pore-forming α_{1A} subunit (Buraei and Yang 2010), (2) Ca²⁺-calmodulin binding to the IQ-like motif at the α_{1A} C-tail (DeMaria et al. 2001; Cens et al. 2006; this report), and (3) syntaxin-1A, quite possibly, via its binding to the *synprint* site at the intracellular loop between domains II and III (LII-III) of α_{1A} (Sheng et al. 1994, 1997; Rettig et al. 1996; Kim and Caterall 1997; Jarvis et al. 2002).

As previously reported for fast inactivation (Lee et al. 2000), we observed a substantial Ca²⁺-dependent component in the steady-state inactivation of Ca_v2.1 only in the presence of the palmitoylated, membrane-anchored β_{2a} subunit (which, contrary to other regulatory β subunits (such as β_1 or β_3), reduces voltage-dependent inactivation (Birnbaumer et al. 1998)). In agreement with findings

from DeMaria et al. (2001) on Ca_v2.1 fast inactivation, the Ca²⁺-dependent component of the steady-state slow inactivation required the Ca²⁺-calmodulin-binding IQ-like motif, with no detectable role of the previously involved CBD site (Lee et al. 2000). Hence, Ca_v2.1 Ca²⁺-dependent steady-state inactivation was abolished by the introduction of the double mutation IM/EE at the IQ-like motif, but unaffected by a truncation of the α_{1A} C-tail, downstream the IQ-like motif, that fully removes the CBD site. Besides, the Ca²⁺-dependent component of Ca_v2.1 steady-state inactivation seems to depend also on specific conformational changes induced by the binding of the functionally different β subunits at the α_{1A} LI-II. Thus, the introduction of a LI-II deletion (Δ LI-II_{451–457}) downstream the AID, around the A454 residue (of relevance for the modulation of Ca_v2.1 inactivation by β subunits and SNAREs (Serra et al. 2010)), made Ca²⁺-sensitive the steady-state inactivation of β_3 -containing Ca_v2.1 channels. Such Ca_v2.1 LI-II deletion affects a fragment of a poorly conserved LI-II region of 13 amino acids that in the cardiac Ca_v1.2 channel can bind Ca²⁺-calmodulin (Pitt et al. 2001) (Fig. 8). Still, removal of this Ca_v1.2 region (Δ LI-II_{520–532}) did not abolish the Ca²⁺-dependent component of cardiac channel inactivation (Pitt et al. 2001). This result agrees with our observation that Δ LI-II_{451–457} had no effect on the Ca²⁺-dependent inactivation of Ca_v2.1 channels containing the β_{2a} subunit.

Interestingly, syntaxin-1A was only able to modulate Ca_v2.1 steady-state inactivation when the Ca²⁺-dependent component was absent either because of the presence of β_3 in a channel formed by a α_{1A} subunit with unaltered LI-II, or due to the removal of channel Ca²⁺-sensitivity by high intracellular Ca²⁺ buffering or by mutation of the IQ-like motif.

Whether the above described functional cross talk is due to a three-dimensional rearrangement of the involved α_{1A} intracellular domains (i.e., LI-II, LII-III and C-tail), and the subsequent alteration of the interaction pattern between them and/or with their interacting partners (regulatory β subunits, SNARE proteins, and the Ca²⁺-calmodulin complex), remains to be elucidated. However, there is evidence that make this hypothesis plausible since it has been reported that N-tail, intracellular loop between domains III and IV (LIII-IV) and C-tail regions of Ca_v2.x or Ca_v1.2 α_1 subunits modulate channel inactivation through direct and dynamic interactions with LI-II, or indirectly via regulatory β subunits (Geib et al. 2002; Kim et al. 2004; Stotz et al. 2004). To date, there are no structural data regarding the whole Ca_v2.1 channel complex that allow us to confirm these physical interactions between α_{1A} cytoplasmic domains. Nevertheless, the cryo-electron microscopy (cryo-EM) structure of the rabbit Ca_v1.1 complex, containing the pore-forming α_{1S} and the

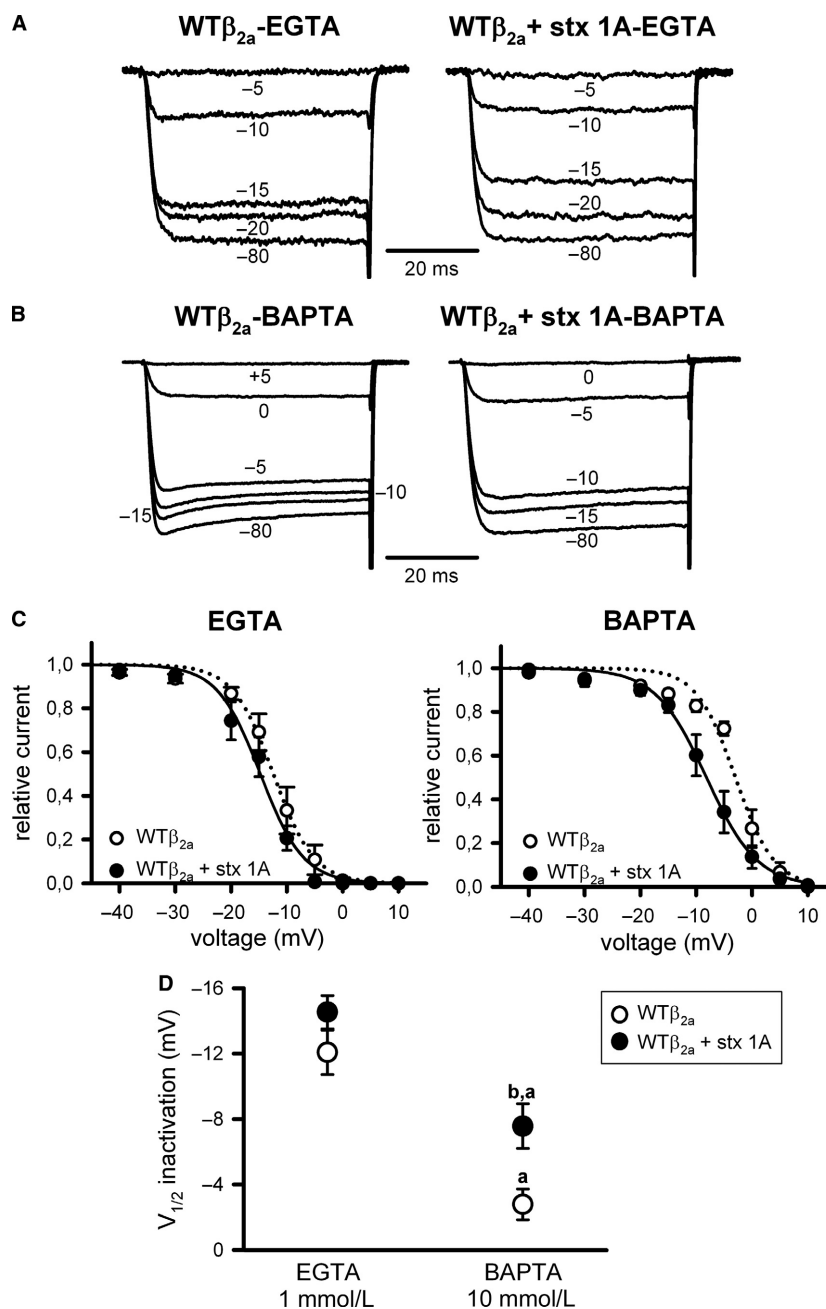


Figure 4. Steady-state inactivation of Ca_v2.1 channels containing the regulatory β_{2a} subunit presents a Ca²⁺-dependent component and no regulation by syntaxin-1A. Illustrative normalized Ca²⁺ current traces recorded at intermediate (1 mmol/L EGTA) (A) or high (10 mmol/L BAPTA) (B) intracellular Ca²⁺-buffering conditions from a HEK 293 cell expressing Ca_v2.1 channels composed of WT α_{1A} , β_{2a} , and $\alpha_2\delta$ subunits (WT β_{2a}) either in the absence (left) or presence (right) of syntaxin-1A (stx 1A). Currents were elicited by 50-ms depolarizing steps to +20 mV applied after 30-sec depolarizing prepulses to the indicated voltages. Corresponding mean normalized steady-state inactivation curves (C), and estimated $V_{1/2}$ inactivation (D) for Δ LI-II₄₅₁₋₄₅₇ Ca_v2.1 mutant channels containing the β_{2a} subunit (WT β_{2a}) in the absence (open circles) or presence (filled circles) of syntaxin-1A (stx 1A), at the above indicated intracellular Ca²⁺-buffering conditions. Average $V_{1/2}$ inact and k_{inact} values at intermediate Ca²⁺-buffering condition (1 mmol/L EGTA) were (in mV): WT β_{2a} (open circles, $n = 12$) -12.08 ± 1.36 and -2.43 ± 0.41 ; WT β_{2a} + stx 1A (filled circles, $n = 11$) -14.53 ± 1.02 and -2.33 ± 0.28 , respectively. At high Ca²⁺-buffering condition (10 mmol/L BAPTA), average $V_{1/2}$ inact and k_{inact} values were (in mV): WT β_{2a} (open circles, $n = 9$) -2.78 ± 0.95 and -3.1 ± 0.52 ; WT β_{2a} + stx 1A (filled circles, $n = 11$) -7.57 ± 1.36 and -3.15 ± 0.55 , respectively. a: $P < 0.001$ when compared to the intermediate Ca²⁺-buffering condition (1 mmol/L EGTA); b: $P < 0.05$ versus the corresponding control condition (absence of syntaxin-1A). No significant difference was found for k_{inact} values (ANOVA $P = 0.44$).

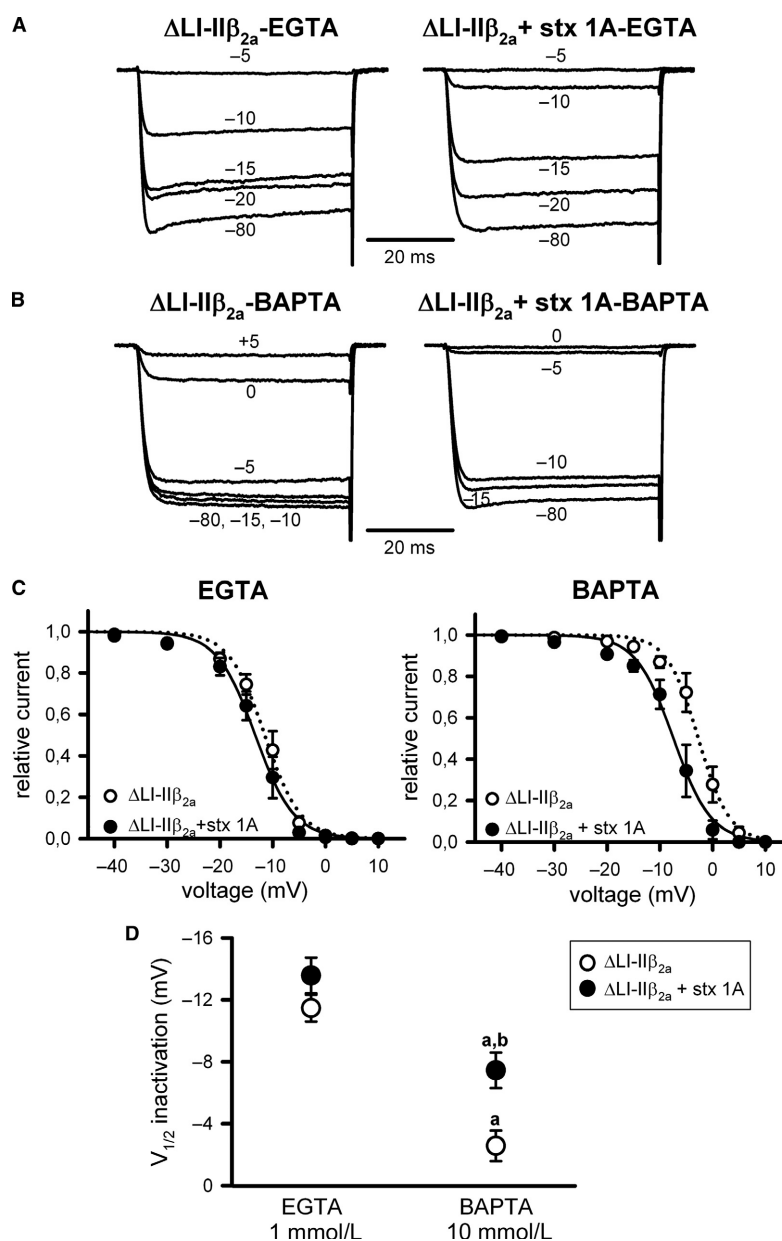


Figure 5. Steady-state inactivation of Ca_v2.1 channels formed by mutant α_{1A} Δ LI-II₄₅₁₋₄₅₇ and β_{2a} subunits remains Ca²⁺-dependent and syntaxin-1A-insensitive. Representative normalized Ca²⁺ current traces recorded at intermediate (1 mmol/L EGTA) (A) or high (10 mmol/L BAPTA) (B) intracellular Ca²⁺-buffering conditions from a HEK 293 cell expressing Ca_v2.1 channels composed of mutant Δ LI-II₄₅₁₋₄₅₇ α_{1A} , β_{2a} , and $\alpha_2\delta$ subunits (Δ LI-II β_{2a}) either in the absence (left) or presence (right) of syntaxin-1A (stx 1A). Currents were elicited by 50-ms depolarizing steps to +20 mV applied after 30-sec depolarizing prepulses to the indicated voltages. Amplitudes of currents elicited by test pulses to +20 mV after the different prepulses were normalized to the maximum current amplitude obtained after a 30-sec prepulse to -80 mV in order to generate the corresponding mean steady-state inactivation curves (C), which were fitted to a single Boltzmann function (see Methods, eq. 1) to estimate the half-inactivation potentials ($V_{1/2}$ inactivation) (D) for mutant Δ LI-II₄₅₁₋₄₅₇ Ca_v2.1 mutant channels containing the β_{2a} subunit (Δ LI-II β_{2a}) in the absence (open circles) or presence (filled circles) of syntaxin-1A (stx 1A), at the above indicated intracellular Ca²⁺-buffering conditions. Average $V_{1/2}$ inact and k_{inact} values at intermediate Ca²⁺-buffering condition (1 mmol/L EGTA) were (in mV): Δ LI-II β_{2a} (open circles, $n = 8$) -11.47 ± 0.86 and -2.87 ± 0.5 ; Δ LI-II β_{2a} + stx 1A (filled circles, $n = 9$) -13.57 ± 1.15 and -2.73 ± 0.44 , respectively. At high Ca²⁺-buffering condition (10 mmol/L BAPTA), average $V_{1/2}$ inact and k_{inact} values were (in mV): Δ LI-II β_{2a} (open circles, $n = 9$) -2.58 ± 0.99 and -2.05 ± 0.43 ; Δ LI-II β_{2a} + stx 1A (filled circles, $n = 9$) -7.45 ± 1.15 and -2.12 ± 0.51 , respectively. a: $P < 0.001$ when compared to the intermediate Ca²⁺-buffering condition (1 mmol/L EGTA); b: $P < 0.01$ versus the corresponding control condition (absence of syntaxin-1A). No significant difference was found for k_{inact} values (ANOVA $P = 0.51$).

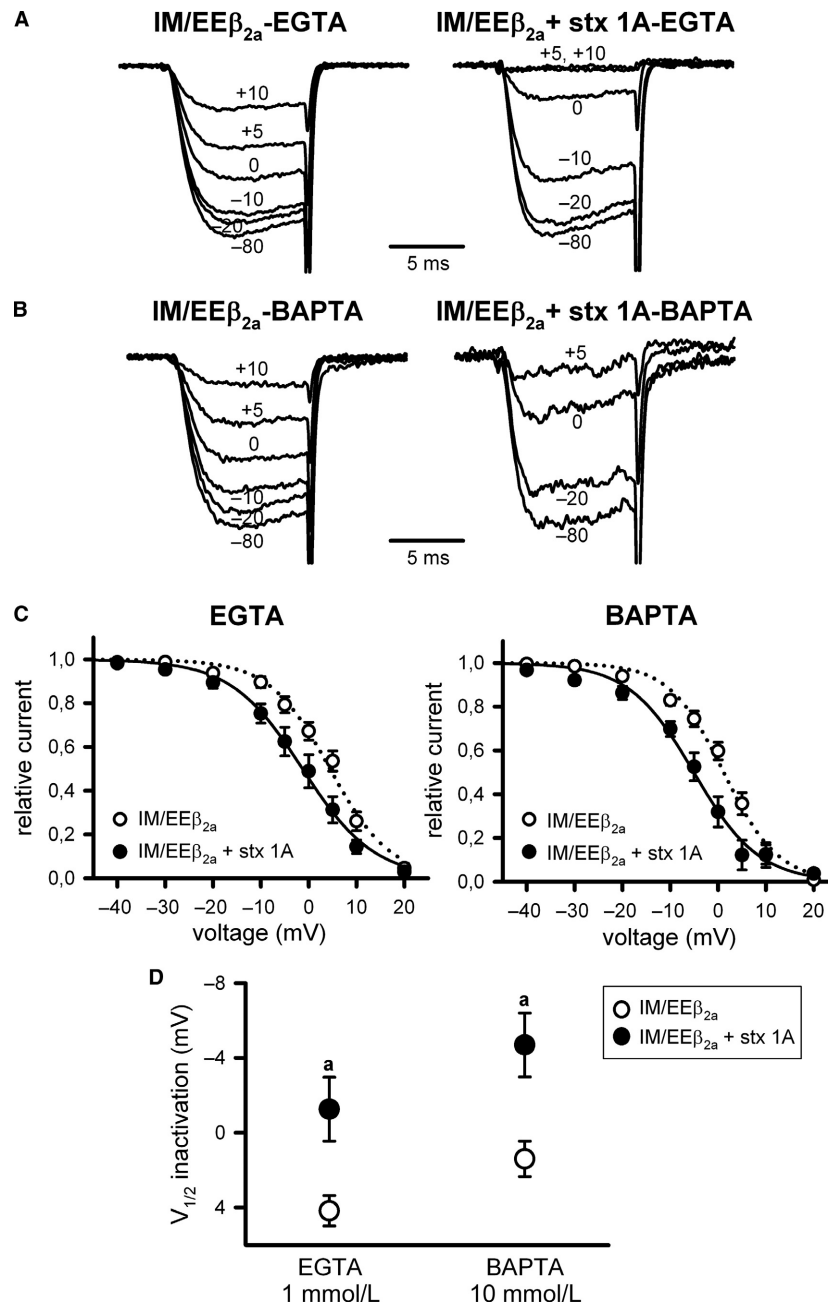


Figure 6. α_{1A} IQ-like motif mutation (IM/EE) remove the Ca²⁺-dependent component in the steady-state inactivation of β_{2a} -containing Ca_v2.1 channels, and it allows modulation by syntaxin-1A. Representative normalized Ca²⁺ current traces recorded at intermediate (1 mmol/L EGTA) (A) or high (10 mmol/L BAPTA) (B) intracellular Ca²⁺-buffering conditions from a HEK 293 cell expressing Ca_v2.1 channels composed of mutant IM/EE α_{1A} , β_{2a} , and $\alpha_2\delta$ subunits (IM/EE β_{2a}) either in the absence (left) or presence (right) of syntaxin-1A (stx 1A). Currents were elicited by 10-ms depolarizing steps to +20 mV applied after 30-sec depolarizing prepulses to the shown voltages. Corresponding mean normalized steady-state inactivation curves (C), and derived V_{1/2} inactivation (D) for IM/EE Ca_v2.1 mutant channels containing the β_{2a} subunit (IM/EE β_{2a}) in the absence (open circles) or presence (filled circles) of syntaxin-1A (stx 1A), at the above indicated intracellular Ca²⁺-buffering conditions. Average V_{1/2} inact and k_{inact} values at intermediate Ca²⁺-buffering condition (1 mmol/L EGTA) were (in mV): IM/EE β_{2a} (open circles, n = 10) 4.19 ± 0.8 and -6.17 ± 0.5; IM/EE β_{2a} + stx 1A (filled circles, n = 11) -1.25 ± 1.71 and -6.44 ± 0.34, respectively. At high Ca²⁺-buffering condition (10 mmol/L BAPTA), average V_{1/2} inact and k_{inact} values were (in mV): IM/EE β_{2a} (open circles, n = 7) 1.4 ± 0.95 and -5.8 ± 0.62; IM/EE β_{2a} + stx 1A (filled circles, n = 9) -4.68 ± 1.71 and -6.21 ± 0.42, respectively. a: P < 0.05 versus the corresponding control condition (absence of syntaxin-1A). No significant difference was found for k_{inact} values (ANOVA P = 0.82).

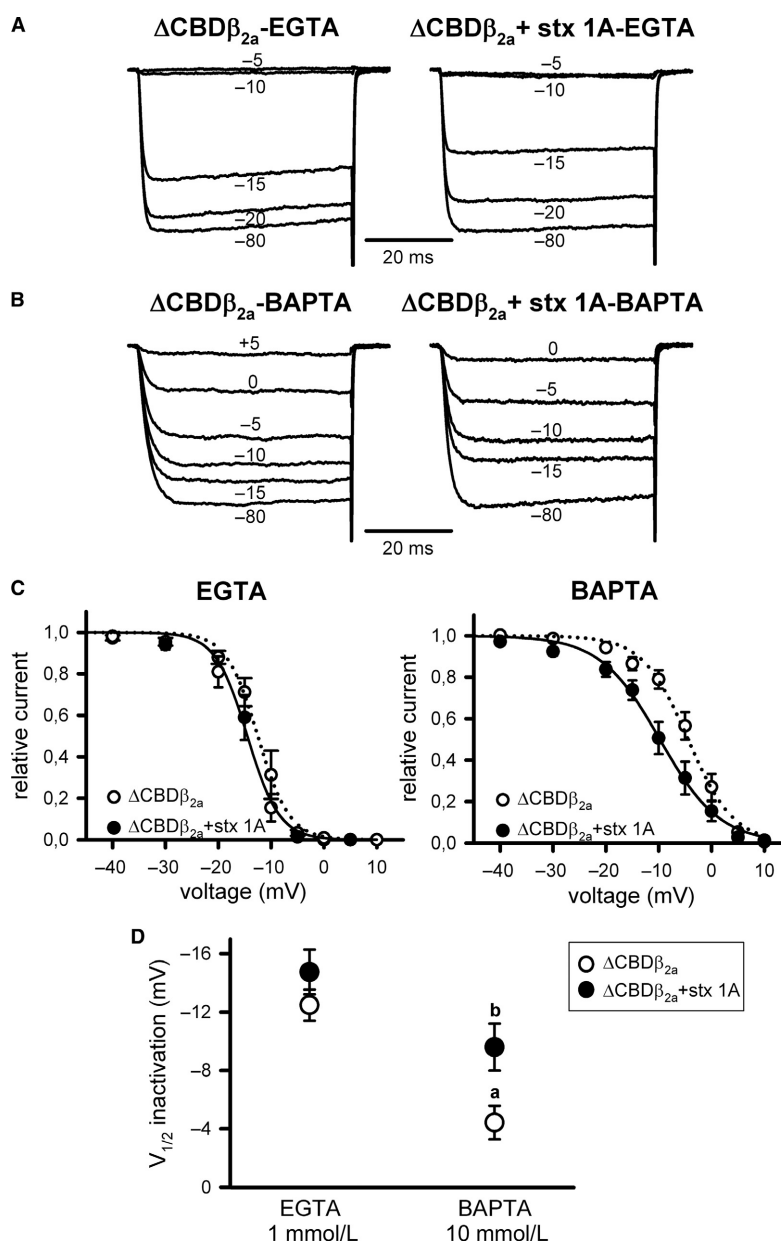


Figure 7. Steady-state inactivation of Ca_v2.1 channels formed by mutant α_{1A} Δ CBD and β_{2a} subunits still shows a Ca²⁺-dependent component and no regulation by syntaxin-1A. Typical normalized Ca²⁺ current traces recorded at intermediate (1 mmol/L EGTA) (A) or high (10 mmol/L BAPTA) (B) intracellular Ca²⁺-buffering conditions from a HEK 293 cell expressing Ca_v2.1 channels composed of mutant Δ CBD α_{1A} , β_{2a} , and $\alpha_{2\delta}$ subunits (Δ CBD β_{2a}) either in the absence (left) or presence (right) of syntaxin-1A (stx 1A). Currents were elicited by 50-ms depolarizing steps to +20 mV applied after 30-sec depolarizing prepulses to the shown voltages. Corresponding mean normalized steady-state inactivation curves (C), and derived $V_{1/2}$ inactivation (D) for Δ CBD Ca_v2.1 mutant channels containing the β_{2a} subunit (Δ CBD β_{2a}) in the absence (open circles) or presence (filled circles) of syntaxin-1A (stx 1A), at the above indicated intracellular Ca²⁺-buffering conditions. Average $V_{1/2}$ $_{inact}$ and k_{inact} values at intermediate Ca²⁺-buffering condition (1 mmol/L EGTA) were (in mV): Δ CBD β_{2a} (open circles, $n = 8$) -12.48 ± 1.07 and -2.23 ± 0.25 ; Δ CBD β_{2a} + stx 1A (filled circles, $n = 6$) -14.75 ± 1.53 and -2.59 ± 0.31 , respectively. At high Ca²⁺-buffering condition (10 mmol/L BAPTA), average $V_{1/2}$ $_{inact}$ and k_{inact} values were (in mV): Δ CBD β_{2a} (open circles, $n = 12$) -4.43 ± 1.15 and -3.68 ± 0.25 ; Δ CBD β_{2a} + stx 1A (filled circles, $n = 12$) -9.6 ± 1.61 and -4.52 ± 0.5 , respectively. a: $P < 0.01$ when compared to the intermediate Ca²⁺-buffering condition (1 mmol/L EGTA); b: $P < 0.05$ versus the corresponding control condition (absence of syntaxin-1A). k_{inact} values were significantly higher ($P < 0.05$) at high Ca²⁺-buffering condition (10 mmol/L BAPTA) than at intermediate Ca²⁺-buffering condition (1 mmol/L EGTA). The presence of syntaxin-1A had no significant effect on k_{inact} .

regulatory $\alpha_2\delta_1$, β_{1a} , and γ subunits, has been recently resolved with high, near-atomic (3.6 Å) resolution (Wu et al. 2016). The structural analysis provides an atomic model for a potentially inactivated state of the Ca_v1.1 channel. In relation to the three-dimensional arrangement of α_{1S} intracellular domains, the structural data locate the AID motif at LI-II packed in between the regulatory β_{1a} subunit and the voltage sensor of α_{1S} domain II, and shows the formation of a globular helical domain due to the interaction between LIII-IV and the proximal C-tail (upstream the IQ motif) (Wu et al. 2016). The substantial homology between rabbit α_{1S} and human α_{1A} subunits with regard to residues involved in such LIII-IV/C-tail physical interaction (Fig. 9) suggests a similar scenario for the Ca_v2.1 channel. Unfortunately, several cytoplasmic segments were not visible in the cryo-EM structure of Ca_v1.1 α_{1S} subunit, and the structure of LI-II upstream the AID, the whole LII-III and the C-tail after residue D1515 (including the IQ motif) could not be resolved (Wu et al. 2016). Therefore, there are no structural data available neither on the possible interaction of LI-II with either LIII-IV or the C-tail, or on any interaction involving LII-III.

Biochemical experiments with recombinant proteins *in vitro* strongly indicate that the *synprint* site, located at LII-III of $\alpha_{1A/B}$, serves an important anchoring function that may facilitate SNARE's modulation of Ca_v2.1 and Ca_v2.2 gating (Sheng et al. 1994, 1997; Rettig et al. 1996; Kim and Catterall 1997; Jarvis et al. 2002). Nonetheless, functional studies also suggest that the regulatory action of SNAREs might involve binding to other sites in the pore-forming α_1 channel subunit, and LI-II and the C-tail regions have been proposed as candidates (Bezprozvanny et al. 2000; Serra et al. 2010). Supporting this idea, recent findings show that low voltage-activated Ca_v3.x (T-type) α_1 channel subunits, which do not contain the consensus *synprint* site, biochemically interact with syntaxin-1A and SNAP-25 at the carboxy-terminal domain (Weiss et al. 2012). In particular, syntaxin-1A binding to Ca_v3.x channels potently modulates channel gating in a similar way that found for Ca_v2.x channels (Weiss et al. 2012). Besides, Ca_v3.x-SNAREs interaction also appears essential for T-type channel-triggered low-threshold exocytosis (Weiss et al. 2012), thus providing a molecular mechanism for their coupling to neurotransmitter and hormone release in neurons and neuroendocrine cells near resting conditions or during mild stimulations (Carbone et al. 2014).

In conclusion, our data suggest that conformational modifications of α_{1A} LI-II (due to the binding of a particular regulatory β subunit, mutation A454T (Serra et al. 2010), or deletion Δ LI-II_{451–457}) determine the modulation of Ca_v2.1 steady-state inactivation either by Ca²⁺ or by SNAREs but not by both.

Acknowledgments

We are grateful to Dr. J. Striessnig (University of Innsbruck, Austria) for the gift of human *CACNA1A* cDNA and Dr. J. Blasi (Universitat de Barcelona, Spain) for providing syntaxin-1A cDNA. We also thank Dr. L. Birnbaumer (National Institutes of Health, North Carolina, USA) for the gift of the cDNAs encoding rabbit $\alpha_2\delta$, and rat β_{2a} and β_3 regulatory subunits, and Dr. F. Rubio-Moscardó for excellent technical assistance.

Conflict of Interest

The authors declare that no conflict of interests exists.

In memoriam

In memory of Gemma G. Genè, PhD (1977–2017).

References

- Atlas, D. 2013. The voltage-gated calcium channel functions as the molecular switch of synaptic transmission. *Annu. Rev. Biochem.* 82:607–635.
- Bachnoff, N., M. Cohen-Kutner, M. Trus, and D. Atlas. 2013. Intra-membrane signaling between the voltage-gated Ca²⁺-channel and cysteine residues of syntaxin-1A coordinates synchronous release. *Sci. Rep.* 3:1620.
- Bezprozvanny, I., R. H. Scheller, and R. W. Tsien. 1995. Functional impact of syntaxin on gating of N-type and Q-type calcium channels. *Nature* 378:623–626.
- Bezprozvanny, I., P. Zhong, R. H. Scheller, and R. W. Tsien. 2000. Molecular determinants of the functional interaction between syntaxin and N-type Ca²⁺ channel gating. *Proc. Natl Acad. Sci. USA* 97:13943–13948.
- Birnbaumer, L., N. Qin, R. Olcese, E. Tareilus, D. Platano, J. Costantin, et al. 1998. Structures and functions of calcium channel β subunits. *J. Bioenerg. Biomembr.* 30:357–375.
- Buraei, Z., and J. Yang. 2010. The β subunit of voltage-gated Ca²⁺ channels. *Physiol. Rev.* 90:1461–1506.
- Carbone, E., C. Calorio, and D. H. F. Vandael. 2014. T-type channel-mediated neurotransmitter release. *Pflügers Arch – Eur. J. Physiol.* 466:677–687.
- Catterall, W. A. 2011. Voltage-gated calcium channels. *Cold Spring Harb. Perspect. Biol.* 3:a003947.
- Cens, T., M. Rousset, J. P. Leyris, P. Fesquet, and P. Charnet. 2006. Voltage- and calcium-dependent inactivation in high voltage-gated Ca²⁺ channels. *Prog. Biophys. Mol. Biol.* 90:104–117.
- Condliffe, S. B., A. Fratangeli, N. R. Munasinghe, E. Saba, M. Passafaro, C. Montrasio, et al. 2013. The E1015K variant in the *synprint* region of the Ca_v2.1 channel alters channel function and is associated with different migraine phenotypes. *J. Biol. Chem.* 288:33873–33883.

- Cricchi, F., C. Di Lorenzo, G. S. Grieco, C. Rengo, A. Cardinale, M. Racaniello, et al. 2007. Early-onset progressive ataxia associated with the first CACNA1A mutation identified within the I-II loop. *J. Neurol. Sci.* 254:69–71.
- Degtiar, V. E., R. H. Scheller, and R. W. Tsien. 2000. Syntaxin modulation of slow inactivation of N-type calcium channels. *J. Neurosci.* 20:4355–4367.
- DeMaria, C. D., T. W. Soong, B. A. Alseikhan, R. S. Alvania, and D. T. Yue. 2001. Calmodulin bifurcates the local Ca²⁺ signal that modulates P/Q-type Ca²⁺ channels. *Nature* 411:484–489.
- Geib, S., G. Sandoz, V. Cornet, K. Mabrouk, O. Fund-Saunier, D. Bichet, et al. 2002. The interaction between the I-II loop and the III-IV loop of Ca_v2.1 contributes to voltage-dependent inactivation in a β -dependent manner. *J. Biol. Chem.* 277:10003–10013.
- Harkins, A. B., A. L. Cahill, J. F. Powers, A. S. Tischler, and A. P. Fox. 2004. Deletion of the synaptic protein interaction site of the N-type (Ca_v2.2) calcium channel inhibits secretion in mouse pheochromocytoma cells. *Proc. Natl Acad. Sci. USA* 101:15219–15224.
- Jarvis, S. E., W. Barr, Z. P. Feng, J. Hamid, and G. W. Zamponi. 2002. Molecular determinants of syntaxin 1 modulation of N-type calcium channels. *J. Biol. Chem.* 277:44399–44407.
- Keith, R. K., R. E. Poage, C. T. Yokoyama, W. A. Catterall, and S. D. Meriney. 2007. Bidirectional modulation of transmitter release by calcium channel/syntaxin interactions in vivo. *J. Neurosci.* 27:265–269.
- Kim, D. K., and W. A. Catterall. 1997. Ca²⁺-dependent and -independent interactions of the isoforms of the α 1A subunit of brain Ca²⁺ channels with presynaptic SNARE proteins. *Proc. Natl Acad. Sci. USA* 94:14782–14786.
- Kim, J., S. Ghosh, D. A. Nunziato, and G. S. Pitt. 2004. Identification of the components controlling inactivation of voltage-gated Ca²⁺ channels. *Neuron* 41:745–754.
- Lee, A., T. Scheuer, and W. A. Catterall. 2000. Ca²⁺/calmodulin-dependent facilitation and inactivation of P/Q-type Ca²⁺ channels. *J. Neurosci.* 20:6830–6838.
- Mochida, S., Z. H. Sheng, C. Baker, H. Kobayashi, and W. A. Catterall. 1996. Inhibition of neurotransmission by peptides containing the synaptic protein interaction site of N-type Ca²⁺ channels. *Neuron* 17:781–788.
- Mochida, S., R. E. Westenbroek, C. T. Yokoyama, H. Zhong, S. J. Myers, T. Scheuer, et al. 2003. Requirement for the synaptic protein interaction site for reconstitution of synaptic transmission by P/Q-type calcium channels. *Proc. Natl Acad. Sci. USA* 100:2819–2824.
- Nanoua, E., T. Scheuera, and W. A. Catterall. 2016. Calcium sensor regulation of the Ca_v2.1 Ca²⁺ channel contributes to long-term potentiation and spatial learning. *Proc. Natl Acad. Sci. USA* 113:13209–13214.
- Pitt, G. S., R. D. Zühlke, A. Hudmon, H. Schulman, H. Reuter, and R. W. Tsien. 2001. Molecular basis of calmodulin tethering and Ca²⁺-dependent inactivation of L-type Ca²⁺ channels. *J. Biol. Chem.* 276:30794–30802.
- Rettig, J., Z. H. Sheng, D. K. Kim, C. D. Hodson, T. P. Snutch, and W. A. Catterall. 1996. Isoform-specific interaction of the α 1A subunits of brain Ca²⁺ channels with the presynaptic proteins syntaxin and SNAP-25. *Proc. Natl Acad. Sci. USA* 93:7363–7368.
- Rettig, J., C. Heinemann, U. Ashery, Z. H. Sheng, C. T. Yokoyama, W. A. Catterall, et al. 1997. Alteration of Ca²⁺ dependence of neurotransmitter release by disruption of Ca²⁺ channel/syntaxin interaction. *J. Neurosci.* 17:6647–6656.
- Serra, S. A., E. Cuenca-León, A. Llobet, F. Rubio-Moscardo, C. Plata, O. Carreño, et al. 2010. A mutation in the first intracellular loop of CACNA1A prevents P/Q channel modulation by SNARE proteins and lowers exocytosis. *Proc. Natl Acad. Sci. USA* 107:1672–1677.
- Sheng, Z. H., J. Rettig, M. Takahashi, and W. A. Catterall. 1994. Identification of a syntaxin-binding site on N-type calcium channels. *Neuron* 13:1303–1313.
- Sheng, Z. H., C. T. Yokoyama, and W. A. Catterall. 1997. Interaction of the synprint site of N-type Ca²⁺ channels with the C2B domain of synaptotagmin I. *Proc. Natl Acad. Sci. USA* 94:5405–5410.
- Stotz, S. C., S. E. Jarvis, and G. W. Zamponi. 2004. Functional roles of cytoplasmic loops and pore lining transmembrane helices in the voltage-dependent inactivation of HVA calcium channels. *J. Physiol.* 554:263–273.
- Weiss, N., S. Hameed, J. M. Fernández-Fernández, K. Fablet, M. Karmazinova, C. Poillot, et al. 2012. A Ca_v3.2/syntaxin-1A signaling complex controls T-type channel activity and low-threshold exocytosis. *J. Biol. Chem.* 287:2810–2818.
- Wu, J., Z. Yan, Z. Li, X. Qian, S. Lu, M. Dong, et al. 2016. Structure of the voltage-gated calcium channel Ca_v1.1 at 3.6 Å resolution. *Nature* 537:191–196.
- Zamponi, G. W. 2003. Regulation of presynaptic calcium channels by synaptic proteins. *J. Pharmacol. Sci.* 92:79–83.
- Zhong, H., C. T. Yokoyama, T. Scheuer, and W. A. Catterall. 1999. Reciprocal regulation of P/Q-type Ca²⁺ channels by SNAP-25, syntaxin and synaptotagmin. *Nat. Neurosci.* 2:939–941.